

Enhanced Generalized OFDM with Index Modulation

A.Atef Ibrahim, Amr A.Nagy, Ashraf Mahran, Amr Abdelaziz
 Department of communication, Military Technical College, Cairo, Egypt.
 ahmedatef1982@hotmail.com, amr.a.nagy@mtc.edu.eg

Abstract—In recent years, many attempts have been made to enhance Orthogonal Frequency Multiplexing with Index Modulation (OFDM-IM) in terms of spectral efficiency and error performance. Two challenges typically erupt when using OFDM-IM. First, the degradation in spectral efficiency due to the subcarrier’s deactivation, especially when using higher order modulation (M-ary) where every inactive subcarrier will cost $\log_2(M)$ bits loss. Second, using a fixed number of active subcarriers within a sub-block forces the error to be localized within the sub-block. Yet, it loses the advantage of exploiting all possible pattern combinations degrading the overall spectral efficiency. In this paper, we introduce a solution to tackle those problems. The Enhanced Generalized Index Modulation (EGIM) is a simple systematic way to generate and detect the OFDM-IM frame. Unlike the classical OFDM-IM generation by splitting the frame into sub-frames which increases the complexity of the OFDM-IM transmitter and reflects on the receiver Maximum likelihood detector, EGIM Makes full use of all possible combinations of active subcarriers within the frame by using variable active subcarriers (k) depending on the incoming data. The EGIM is still susceptible to error propagation if the OFF symbol is wrongly mapped to one of the ON symbols or vice versa. For that reason, we offer an OFDM-IM autoencoder to overcome this problem. The encoder generates the (ON/OFF) symbols systematically to achieve the advantage of sending all possible frame indices patterns depending on the input bit stream offering an average of 3dB gain in terms of power efficiency. The proposed encoder performance was compared to the standard encoder with the same effective coding rate using soft and hard decision Viterbi decoding utilizing the power gain achieved.

Index Terms—Enhanced Generalized OFDM With Index Modulation, In-phase/Quadrature IM, Spectral Efficiency, Error Propagation, OFDM-IM autoencoder.

I. INTRODUCTION

THE idea of index modulation is first introduced in [1] as a technique to enhance the spectral efficiency of multi-carrier communication systems over frequency-selective and rapidly time-varying fading channels, transmitting additional bits through activating and deactivating data subcarriers within data sub-block which creates a new domain of transmitting data (index domain). Dividing the OFDM frame into multiple sub-blocks using low order modulation (BPSK) symbols boosts spectral

efficiency to exceed that of the classical OFDM. Yet, there are some points to be investigated:

- 1) Performance evaluation of general M-ary signal constellations.
- 2) Choosing the optimal value of active sub-carrier k and total number of bits for each sub-block n .

Both factors negatively affect the spectral efficiency of IM communication systems as follows:

- 1) The deactivation of the subcarrier using high order modulation will cause a loss of $\log_2(M)$ bits per subcarrier.
- 2) The best selection of (n, k) to obtain the maximum spectral efficiency of the communication system where n is the number of bits within the subframe.

The work in [1] tries to solve the problems that emerge in the early trials of using the index as a new domain for sending data as follows :

- 1) In [2] subcarrier indices used for data transmission with a high probability of error propagation if the receiver misses the correct indices positions.
- 2) The error propagation problem is solved in [3] by using fixed $k = \frac{N}{2}$, this prevents the error from propagation outside the frame boundaries but leads to huge computational complexity at the receiver to detect which index pattern was sent.

Many problems are still challenging in OFDM-IM communication systems can be summarized as follows:

The complexity of the receiver detector: This results from the large number of index patterns the receiver is required to distinguish(e.g.: in [3] there is $C_{\frac{N}{2}}^N$), the problem was solved by dividing the frame into many sub-frames so that the receiver has low allowable patterns to detect. However, this will limit spectral efficiency results of the system comes from the index pattern combinations term $\lfloor \log_2 C_k^n \rfloor$ due to the reduction in C_k^n function from N to n .

The optimal activation ratio for maximum spectral efficiency: hard efforts have been made in [?] in the derivation of the closed form of maximum entropy for an OFDM-IM communication system.

Using a variable number of active subcarriers over the whole frame length with high-order modulation:

on one hand, all possible pattern combinations will be available for the index domain. on the other hand, due to the lack of receiver knowledge of the number of active indices, the error in determining the number and position of active subcarriers within the frame causes the errors to propagate across the OFDM-IM frames [2].

Finally, there is a critical need to enhance the generalization of the OFDM-IM schemes to accommodate all combination patterns while maintaining the low complexity of ML detection at the receiver. Simultaneously, a comprehensive solution for the error propagation problem is crucial to allow the practical application of the OFDM-IM system.

Different forms of IM suited for MIMO and Multicarrier communication systems were mentioned in [4] and [5]. Additionally, an outstanding work on the generalization of OFDM-IM was proposed in [6] where two main techniques were proposed:

- 1) GIM-1 used for BPSK where, the number of the active index is taken from a set of allowable number $K = \{k_1, k_2, \dots, k_r\}$. where r is the size of the index set size, with extreme case $K = \{0, 1, \dots, n\}$ which enhances the spectral efficiency over the classical OFDM-IM.
- 2) GIM-2 higher order modulation (QPSK) is implemented over OFDM-IM without loss of spectral efficiency by considering the in-phase and quadrature components as two independent BPSK streams. The index modulation is applied to the in-phase and quadrature data independently.

Both techniques (GIM-1 and GIM-2) exceed the classical OFDM-IM in terms of spectral efficiency. Additionally, wherever the existence of equality in spectral efficiency the simulations show that the above-mentioned techniques outperform the classical OFDM-IM in bit error rate overall the entire signal-to-noise ratio (SNR). This comes over the expenses of the computational complexity in the log-likelihood ratio (LLR) or Maximum likelihood (ML) detector, the complex multiplication in classical OFDM-IM is $O(M)$ per subcarrier. However, the complexity in GIM1 is $O(rMn)$ and GIM2 is $O(2M)$ per subcarrier. The authors didn't deal with the effect of error propagation of GIM-3 (a combination of GIM-1 and GIM-2) for errors in indices position caused by channel conditions.

Based on the previous concept the technique of OFDM with in-phase/quadrature index modulation (OFDM-I/Q-IM) was presented in [7] and [8]. It can be considered one of the best candidates for high-speed communications [9], where the activation of in-phase and quadrature components occurs independently resulting in higher spectral efficiency (index bits activate Both I and Q components).

The work in [10] presented two additional schemes using higher-order modulation:

- 1) OFDM-HIQ-IM where the in-phase and quadrature components are jointly activated with index selection bits treated independently as two different streams sending different index patterns on the I and Q components.
- 2) LP-OFDM-IQ-IM spreads information symbols across two adjacent active subcarriers through linear constellation precoding 2×2 matrix to achieve additional diversity gain.

Efforts in [11] were made to enhance the spectral efficiency by using adaptive mapping for each picked-up value selected from a set of allowable active indices (e.g. for the low number of active indices choose higher order modulation mapping and vice versa).

In the DM-OFDM-IM technique in [12] and [13] the process of activation and deactivation of the subcarrier takes place by switching between two mapping schemes, the problem in this approach is that the minimum Euclidean distance between symbols is quietly reduced to a small value thus, more power has to invested to achieve reasonable error performance. Where the chance of error propagation still exists, especially in low SNR.

The most recent generalized scheme introduced in [14] where each data sub-block has a different number of active subcarriers (k), associated with Modulation Mode (MM), the active subcarrier number k_r will be picked up from the K set with size R . Where,

$$K = \{k_1, k_2, \dots, k_r, \dots, k_R\} \forall 1 \leq r \leq R, 1 \leq k_r \leq n.$$

For achieving the full degree of freedom of the OFDM-IM frame pattern combinations, it is required to involve all possible combinations of a pattern generated by the C_k^N function, this is valid when the value of $k = N/2$, this can be fulfilled by consider the k as a random variable whose Binomial distribution with mean $N/2$. Due to the lack of knowledge of the number of active subcarriers, any error in determining the position of active subcarriers uploaded by higher-order modulation symbols will cause errors to propagate within the boundaries of the frame affecting all successive frames.

This paper generalizes the use of OFDM-IM over the whole OFDM frame without splitting. This takes advantage of the maximum indices pattern combinations and reduces the transmitter complexity where there are no look-up tables for index selection within the sub-frame. The presented EGIM uses a variable number of active subcarriers in each frame to involve all possible pattern combinations within the whole frame length. More importantly, EGIM can be considered as a pivotal solution to the error propagation problem that emerges when using variable number active indices, k , in OFDM-IM through a customized convolutional encoder whose output is mapped into (ON/OFF) symbols covering all possible pattern combinations while, in addition, taking advantage of its error-correcting capabilities.

The contributions of this work can be summarized as follows:

- 1) A solution for using high-order modulation with a variable number of active indices over the whole OFDM-IM frame without a dramatic loss in spectral efficiency through the use of a variable number of active index k with average value $\frac{N}{2}$, instead of using of fixed (n,k) pair.
- 2) The Design and performance evaluation of EGIM technique where two Case studies were introduced using a systematic way to generate and detect OFDM-IM without splitting and reassembling the frame, as it is implemented without extra complexity computation were added to both techniques (the same as the classical OFDM).
- 3) The design Of OFDM-IM autoencoder generates active and inactive symbols simultaneously utilizing convolutional encoder error capabilities to eliminate error propagation within OFDM-IM frames.

The two case studies of EGIM are:

- a) **The EGIM-4QAM** where the input bit stream is converted into active and inactive symbols uploaded over OFDM frame depending on the input data. The transmitted symbols for active subcarriers are drawn from the normal 4QAM constellation and the inactive subcarrier is sent with zero power (i.e.: $0+j0$).
- b) **The EGIM-8PSK** is a modified version of DM-OFDM introduced in [12], where the two 4QAM schemes (M_A, M_B) is replaced with 8PSK scheme for active subcarriers, also OFF symbol inserted for inactive subcarriers.

The rest of the paper is organized as follows, in section II a brief background of classical OFDM-IM is presented where the main idea of OFDM-IM is explained. In section III, the proposed EGIM technique was depicted with a detailed illustration for its two case studies with the derivation of the spectral efficiency and symbol error performance formulas. The OFDM-IM autoencoder is depicted in section IV. Simulation results are presented and analyzed in section V. Finally, the conclusion of the paper is given in section VI.

II. BACKGROUND ON OFDM-IM

Fig.1 shows the system model of classical OFDM-IM introduced in [1], where the input bit stream B is split into many groups G , i.e.: $B=pG$. Where p is the number of bits per group, similarly the OFDM frame length is divided into smaller groups $N=nG$. there is k number of active subcarrier within the group such that $k \leq n$. The p bits are split into two sections i.e.: $p = p_1 + p_2$, the first one p_1 is used for the index selection pattern I . However, the second p_2 is mapped to a symbol S uploaded on the active index.

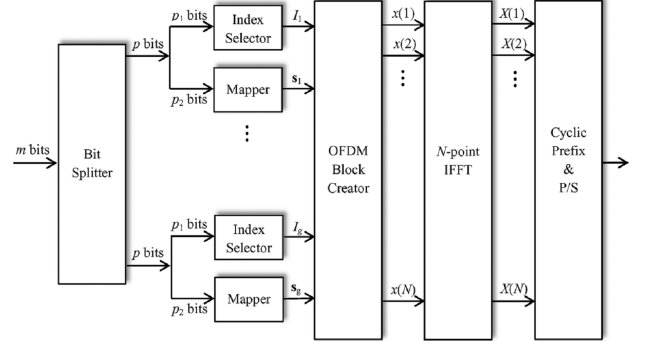


Fig. 1. Classical OFDM-IM transmitter introduced in [1].

The maximum achievable bits gained by selecting k active index out of the number of bits in the group n are:

$$B_1 = p_1 G = \lfloor \log_2 C_k^n \rfloor G. \quad (1)$$

While the maximum achievable bits gained by mapping bits over higher-order modulation

$$B_2 = p_2 G = k(\log_2 M)G. \quad (2)$$

Resulting total achievable bits per OFDM-IM frame:

$$B = B_1 + B_2 = \lfloor \log_2 C_k^n \rfloor G + k \log_2 M G. \quad (3)$$

Recombine both types of bits to form OFDM-IM frame:

$$X_F = [X(1), X(2), \dots, X(N)]^T. \quad (4)$$

where $X(\alpha) \in 0, S$, is the subcarrier states either inactive or active the last one carries constellation symbol α can take values from $0, \dots, N$. The frame \mathbf{X} is processed as classical OFDM, taking the inverse fast Fourier transform (IFFT) as follows:

$$X_T = \frac{N}{\sqrt{k}} IFFT(X_F) \quad (5)$$

X_T is the time domain representation of OFDM frame, $\frac{N}{\sqrt{k}}$ is the normalization factor to ensure that $E\{X_T^H X_T\} = N$, the receiver operate reversely where normalization factor $\frac{\sqrt{k}}{N}$ is used in FFT process.

One of the key challenges in the detection of OFDM-IM is that the receiver has to detect the active index positions first and then demodulate the symbols carried by those active subcarriers, error emerges when the receiver fails to detect the active indices accurately, it results loss in either pattern and constellation bits. This error can be bounded within OFDM-IM when using fixed values of (n, k) , otherwise (using variable active index each frame or subframe) the error in one frame will propagate across the following successive frames [12] cause error floor over the entire SNR range.

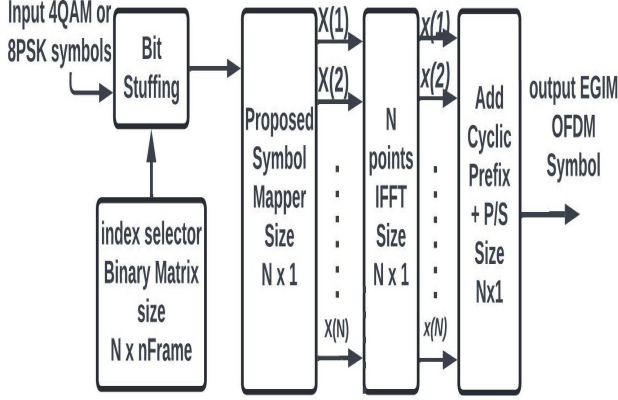


Fig. 2. Equivalent Transmitter of Enhanced Generalized OFDM-IM.

III. ENHANCED GENERALIZED INDEX MODULATION

The EGIM implementation of the IM concept by using a random input stream to determine the number and the index position of active subcarriers within the frame through the Bit stuffing technique which can be described simply as follows:

For a random binary input stream, the resulting output will be as follows:

For "0" input bit the output will be $\log_2 M$ zeros.

For "1" input bit the output will be the input bit followed by $\log_2 M$ bits.

The benefit of this technique is the reduction of error propagation probability, we will deduce the realization of such event later in this paper .

Example: the output for 1101010111100 input over QPSK will be:

Output 110 101 000 111 100.

The above method is equivalent to using N bits stream for index selection where the number of the input binary "1" corresponds to the number and indices of the active subcarrier which carries symbols drawn from the 4QAM constellation as shown in Fig.2 . In other words, the most significant bit in each output symbol corresponds to the index bit. The inactive subcarriers carry the off symbol, the original zero bit stuffed with $\log_2 M$ zeros (i.e.: "00") to preserve the number of bits within a symbol.

A. Spectral Efficiency Analysis

The number of bits per frame that can be sent using QAM/PSK constellation is calculated as follows :

$$B_1 = k \log_2(M) \quad (6)$$

For each frame, the MSB of each symbol represents the N bits for subcarrier activation (index bit), the number of all possible combinations denoted by:

$$B_2 = \lfloor \log_2 C_k^N \rfloor \quad (7)$$

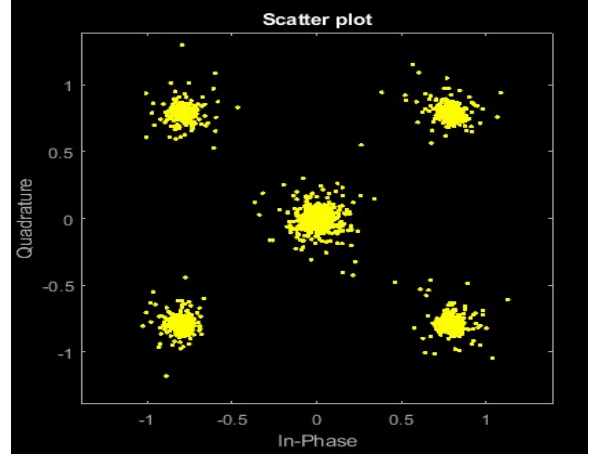


Fig. 3. EGIM-4QAM constellation over AWGN at SNR = 10 dB.

where k is a random variable with Binomial distribution with mean $\frac{N}{2}$ represents the number of active subcarriers

The average spectral efficiency per frame will be :

$$B_{EGIM} = E\{\lfloor \log_2 C_k^N \rfloor + k \log_2(M)\} \quad (8)$$

$$B_{EGIM} = \sum_{k=0}^{k=N} (\log_2 C_k^N + (\frac{N}{2}) \log_2 M) \quad (9)$$

Invoking the log sum inequality, we can write :

$$B_{EGIM} \geq \lfloor \log_2 \sum_{k=0}^{k=N} C_k^N \rfloor + (\frac{N}{2}) \log_2 M \quad (10)$$

The first term is the expansion for 2^N binomial and $\frac{N}{2}$ is the expected value of the active subcarrier random variable, thus the average spectral efficiency per subcarrier will be:

$$B_{EGIM} \geq \frac{1}{N} \lfloor \log_2 2^N \rfloor + (\frac{1}{2}) \log_2 M \quad (11)$$

Therefore the final average spectral efficiency formula per subcarrier for bit stuffing is :

$$B_{EGIM}^{th} \geq 1 + \frac{1}{2} \log_2 M \quad (12)$$

B. The First Case Study 4QAM

The output of the EGIM transmitter in the first case study is limited to five codewords (symbols) are shown in Table I, they are similar to the modified power-saving OFDM policy introduced in [2] described in Fig.3 , a new fifth point is introduced to represent all zero symbols (inactive subcarrier) in addition to the 4QAM constellation.

Although the insertion of the 5th constellation point (origin point) makes the proposed symbol mapper carry (3 bits) instead of (2 bits) in classical 4QAM. The drawback of this technique is that the minimum Euclidean

TABLE I
THE PROPOSED CONSTELLATION FOR THE FIRST CASE STUDY

symbol	code word	constellation
S_o	000	$0 + 0j$
S_1	100	$\frac{1}{\sqrt{2}}(1 + j)$
S_2	110	$\frac{1}{\sqrt{2}}(-1 + j)$
S_3	111	$\frac{1}{\sqrt{2}}(-1 - j)$
S_4	101	$\frac{1}{\sqrt{2}}(1 - j)$

distance between constellation points is reduced from $\sqrt{2}$ unit to 1 unit (assuming normalized power). The result transmitted vector will be:

$$X = [x_1, x_2, \dots, x_N] \text{ where} \quad (13)$$

$$x_i \in \{S_o, \dots, S_4\} \text{ and } i = [1, \dots, N]$$

For our proposed constellation shown in Fig.3 the active carrier to be selected from constellation $M = 4$ and inactive subcarrier carry zero bit, so the SE per subcarrier from (12) will be $B^{th} \geq 2 \text{ bit/subcarrier}$.

However there is little enhancement than the classical (OFDM-4QAM) scheme in terms of spectral efficiency, there is a 3dB saving in terms of power efficiency as the average active subcarrier is $\frac{N}{2}$. In other words, the OFDM symbol is sent with half power.

1) *Error Performance Analysis:* The derivation of the Symbol error rate of EGIM-4QAM is nearly similar to that derived in [2] with two important points that will be mentioned later. The detection of symbols constellation shown in Fig.3 could be divided into two processes:

- The S_o symbol detection is exactly like OOK coherent detection.
- The rest of symbols $\{S_1, S_2, S_3, S_4\}$ will be treated as detection (4QAM) symbols.

The total probability of symbol error in our scheme is the summation of error in inactive indices (ook symbol) and the error in active indices symbol (4-qam) as follows:

$$P_{sym} = P(e/ook)P_{ook} + P(e/qam)P_{qam} \quad (14)$$

$$= \frac{1}{2}P(e/ook) + \frac{1}{2}P(e/qam) \quad (15)$$

where the number of active subcarriers is a random variable Bernoulli distributed with a mean($\frac{N}{2}$), therefore the probability of active subcarriers within the frame is equal to the inactive subcarriers $P(ook) = P(qam) = 0.5$

- 1) The OOK Symbol Error Analysis computed by using the closed form of the symbol error rate of the OOK detector is derived as follows:

$$P(e/ook) = \frac{1}{2} \left(-\sqrt{\frac{0.5\bar{\gamma}_s}{1 + 0.5\bar{\gamma}_s}} \right) \quad (16)$$

The term $\bar{\gamma}_s$ is the average SNR per subcarrier, such that $\bar{\gamma}_s = |\bar{h}_k|^2 \frac{E_s}{N_o}$, where E_s and $|\bar{h}_k|$ is the average energy per symbol and the channel

amplitude respectively. The idea of using half SNR in the above formula is due to the use of half of transmitting power since the inactive indices are sent with no power, the decision region to distinguish between the active and inactive subcarrier is a circle whose center in the origin and radius is equal to the half Euclidean distance between S_o and any other symbol $\{S_1, S_2, S_3, S_4\}$.

- 2) The QAM Symbol Error Analysis computed by using the generalized closed form of symbol error rate probability of detecting QAM (M-ary) symbol over fading channel is derived in [15], we can tailor the result for our scheme presented in section III-B, also mentioned in [2] as follows:

$$P_{qam} = -\frac{1}{8} - \frac{1}{2} \sqrt{\frac{\bar{\gamma}_s}{2 + \bar{\gamma}_s}} + \frac{1}{2\pi} \sqrt{\frac{\bar{\gamma}_s}{2 + \bar{\gamma}_s}} \tan^{-1} \sqrt{\frac{\bar{\gamma}_s}{2 + \bar{\gamma}_s}} \quad (17)$$

The average symbol error probability for EGIM-4QAM scheme introduced in equation (22) derived by substituting with equations (16 and 17) in (14). The result is identical to what is derived in [2]. However, many considerations must be taken into account as follows:

- In [2] the author assumes the independence between B_{ook} (index bits) and B_{QAM} (symbol mapper bits). However, they are correlated, since the resulting errors in B_{ook} will spread out across the frame causing the whole frame error, while in our scheme the error is bounded within symbol bounds for the same case.
- The excess subcarrier that carries the information about the activation pattern depends on the majority of bits (Zeros or Ones), which is also vulnerable to channel error, which will cause total frame error.

C. The Second Case study for EGIM-8PSK

In [12] the symbols are drawn from one of two constellations M_1 and M_2 depending on the activation process.

In this section, we will extend the idea of bit-stuffing introduced section III-B to be applied across the whole frame of DM-OFDM-IM in [12] using 8psk constellation instead of (M_A, M_B) , with insertion of the origin point (0+0j) to carry the off symbol as shown in Figure 5, the complete symbol Mapping proposed in such case:

The equivalent transmitter of EGIM is described in Fig.2 where the input symbols are drawn from the 8PSK constellation. The EGIM-8PSK generation process is depicted in Fig. 4 as follows:

- 1) If the input bit zero is replaced with "0000" the Transmitter jumps the following bits.
- 2) If the input bit is "1" the transmitter investigates the following bit:

TABLE II
PROPOSED MAPPER FOR SECOND CASE STUDY

symbol	code word	constellation
S_o	0000	$0 + 0j$
S_1	1000	$1 + 0j$
S_2	1001	$0 + 1j$
S_3	1010	$-1 + 0j$
S_4	1011	$0 - 1j$
S_5	1100	$\frac{1}{\sqrt{2}}(1 + j)$
S_6	1110	$\frac{1}{\sqrt{2}}(-1 + j)$
S_7	1111	$\frac{1}{\sqrt{2}}(-1 - j)$
S_8	1101	$\frac{1}{\sqrt{2}}(1 - j)$

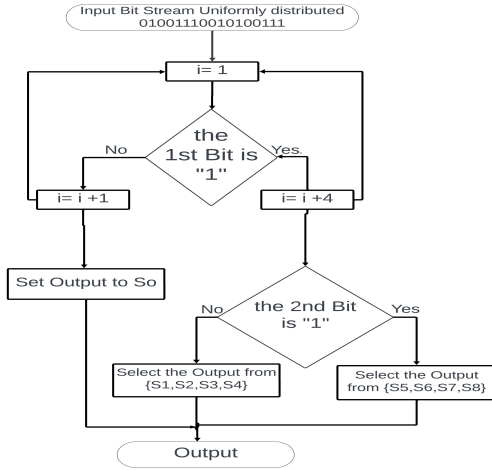


Fig. 4. The Generation of EGIM-8PSK

- Case "0" the output symbol is selected from the M_1 Constellation (i.e. $S \in \{S_1, S_2, S_3, S_4\}$).
- Case "1" the output symbol is selected from the M_2 Constellation (i.e. $S \in \{S_5, S_6, S_7, S_8\}$).

Each of the nine codewords is mapped to in-phase and quadrature components as mentioned in table II. The Major difference between the work introduced in [13] is using an 8PSK Constellation with an additional point inserted with zero power representing the off sub-carriers that enhance the overall spectral efficiency.

D. Spectral Efficiency Analysis

In our case, all symbols $S = S_o, S_1, S_2, \dots, S_8$ within the OFDM frame will be represented by "4bits", the most significant bit in each symbol represents the index pattern, the other 3 bits will depend on the index bit as follows :

- Case "1" the 3 bits will represent constellation points drawn from the 8PSK scheme.

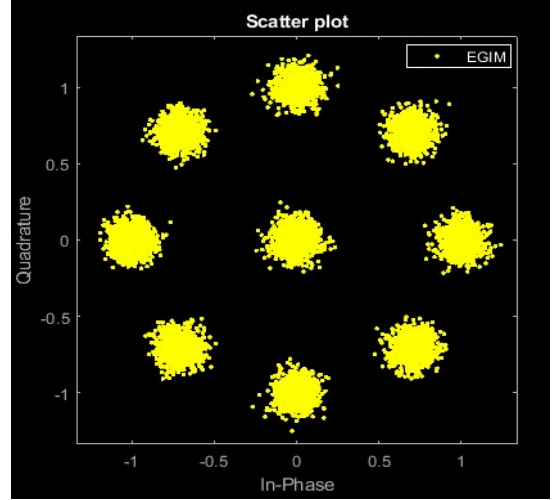


Fig. 5. Modified constellation points 8PSK over AWGN, SNR=20dB

- Case "0" index bit will be followed with "000" to preserve the symbol dimension.

Since symbols are drawn from the 8PSK constellation (i.e. $M=8$), the average spectral efficiency per subcarrier is:

$$B_{8PSK} \geq 1 + \frac{1}{2} \log_2(M). \quad (18)$$

Therefore the number of bits per subcarrier will be:

$$B \geq 2.5 \text{bits}. \quad (19)$$

E. Error Performance Calculation EGIM-8PSK

In this section, we will derive the necessary formulas for the symbol error rate for EGIM-8PSK. For constellation point S_i where $i = 0, 1, \dots, M - 1$. shown in Fig. 5, each points correspond to a symbols as in Table II. The average symbol error rate for the k^{th} subcarrier, where $k = 1, 2, \dots, N$, can be calculated in the same way as in section III-B1 except for using the closed form probability of error of M-PSK instead of the one for M-ary QAM symbols. The symbol error probability of the off symbol will be given by:

$$P(e/ook) = \frac{1}{2} \left(1 - \sqrt{\frac{0.5\bar{\gamma}_s}{1 + 0.5\bar{\gamma}_s}} \right) \quad (20)$$

The closed-form probability of error of M-PSK given in [16] as follows:

$$P_{psk} = \frac{M-1}{M} - \frac{1}{\pi} \sqrt{\frac{\bar{\gamma}_s \sin^2 \frac{\pi}{M}}{1 + \bar{\gamma}_s \sin^2 \frac{\pi}{M}}} \left(\frac{\pi}{2} + \arctan \left(\sqrt{\frac{\bar{\gamma}_s \sin^2 \frac{\pi}{M}}{1 + \bar{\gamma}_s \sin^2 \frac{\pi}{M}}} \right) \cot \frac{\pi}{M} \right) \quad (21)$$

The value of γ is equal to $\frac{1}{N_o}$, where N_o is the variance of noise sample per subcarrier.

TABLE III
SYMBOL ERROR RATE OF EGIM

$$P_{4QAM} = \frac{1}{2} \left[\frac{1}{2} \left(1 - \sqrt{\frac{0.5\gamma_s}{1+0.5\gamma_s}} \right) \right] + \frac{1}{2} \left[\frac{-1}{8} - \left(\frac{1}{2} \right) \sqrt{\frac{\gamma_s}{2+\gamma_s}} + \frac{1}{2\pi} \sqrt{\frac{\gamma_s}{2+\gamma_s}} \tan^{-1} \left(\sqrt{\frac{\gamma_s}{2+\gamma_s}} \right) \right] \quad (22)$$

$$P_{8PSK} = \frac{1}{2} \left[\frac{1}{2} \left(1 - \sqrt{\frac{0.5\gamma_s}{1+0.5\gamma_s}} \right) \right] + \frac{1}{2} \left[\frac{7}{8} - \left(\frac{1}{\pi} \right) \sqrt{\frac{\gamma_s \sin^2(\frac{\pi}{8})}{1+\gamma_s \sin^2(\frac{\pi}{8})}} \left(\frac{\pi}{2} + \tan^{-1} \left(\sqrt{\frac{\gamma_s \sin^2(\frac{\pi}{8})}{1+\gamma_s \sin^2(\frac{\pi}{8})}} \right) \cot \left(\frac{\pi}{8} \right) \right) \right] \quad (23)$$

The total average symbol error rate EGIM-8PSK is listed in equations (23), the reason for computing SER rather than the BER is the huge computational complexity of BER formulas listed in [17] due to the large number of indices pattern the receiver detector have to distinguish.

For the Bit error probability 10^{-3} , a comparison of the two EGIM case study with different forms of IM in terms of received SNR and spectral efficiency per subcarrier is shown in Table IV.

The two cases offer a good choice of error performance

TABLE IV
SPECTRAL EFFICIENCY COMPARISON

scheme	SNR (dB)	bits/subcarrier
EGIM-4QAM	24	≥ 2.5
GIM-2	25	2.75
DM-OFDM-IM	25	2.5
EGIM-8PSK	23	≥ 2
GIM-1	23	1.222

and spectral efficiency. In contrast, the Enhanced generalized techniques have systematic generation and detection at a complexity almost near the classical OFDM system. However, they are also vulnerable to error propagation when OFF-data symbols are wrongly demapped into the ON-symbol and vice versa.

The solution to this problem will be presented in the next section IV, where the error propagation across OFDM-IM frames is avoided by exploiting the error correction capabilities of the proposed OFDM-IM convolutional autoencoder.

IV. IMPLEMENTATION OF OFDM-IM USING AUTOENCODER

This section will demonstrate the generation of error propagation-free OFDM-IM using a customized convolutional encoder, this method will systematically convert the input binary stream into on and off symbols. Additionally, the autoencoder error capabilities prohibit the event of error propagation mentioned in section III-C.

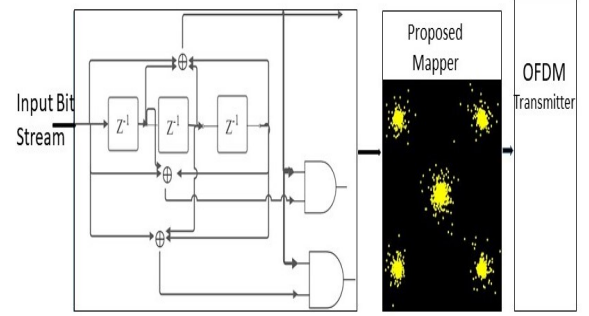


Fig. 6. The structure of OFDM-IM autoencoder

A. Auto Encoder Structure

The proposed autoencoder is depicted in Fig. 6 as a simple convolutional encoder with rate $\frac{1}{3}$ and constraint length of order 4, where its generator polynomials will be as follows:

$$\begin{aligned} g_1(x) &= x^3 + x^2 + x + 1 \\ g_2(x) &= (x^3 + x^2 + x).g_1(x) \\ g_3(x) &= (x^3 + x + 1).g_1(x) \end{aligned}$$

The 1st output is mixed with the 2nd and 3rd with the mean of an And gate which will force the output to all zero symbol (i.e. off symbol) in case the zero is out of 1st generator, On other hands when the 1st output is "1" (i.e. active) allows the encoder to send the constellation symbols. There is a need to define a new term called the effective symbol rate to determine the compared candidate-coded system benchmark as follows:

$$Sym_{eff} = coderate \times \log_2 M. \quad (24)$$

Where the Sym_{eff} of our proposed system (Encoder, Mapper) is "1". The resultant output trellis structure is shown in Fig.7, the encoder systematically maps the input bit stream into five codewords listed in TableI. Where, S_o represents the inactive symbol and the symbols $S_{on} = S_1, S_2, S_3, S_4$ are the active symbols. Hence, the resultant probabilities of the output symbols will be:

$$P_{S_o} = P_{S_{on}} = \frac{1}{2} \quad (25)$$

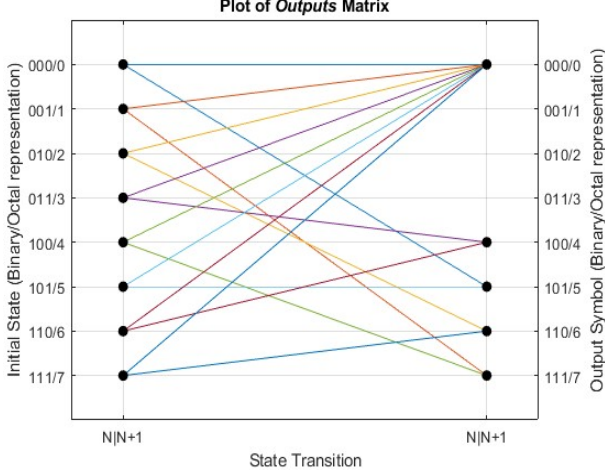


Fig. 7. The output trellis of the OFDM-IM autoencoder

For the input bit stream $[m = m_1, m_2, \dots, m_i]$, the coded output will be:

$$S_i = G(m_i) \text{ where } S_i \in [S_0, \dots, S_4] \quad (26)$$

In the receiver, we employ the Viterbi decoding algorithm with either hard or soft decisions as follows:

B. Hard Decision Decoding

The output bit stream results from the decoder using hard decision Viterbi algorithm follows:

$$d_H = \sum_{i=1}^{tb} |c_i - b_i| \quad (27)$$

Where: d_H is the Hamming distance, c_i is the received bit, b_i is the expected bit and tb is the traceback length (i.e. $tb = 3 \times \text{constraint length}$).

The Viterbi algorithm checks the Hamming distance for all possible paths and selects the route with the minimum distance. Hard decision decoding relies on binary decisions (0 or 1) and compares these to the expected bits to identify and correct errors.

C. Soft Decision Decoding

The decoder input will be samples computed using approximate LLR algorithm in [18] instead of binary input as follows:

$$\mathcal{L}(b) = \frac{-1}{\sigma^2} \left(\min_{s \in S_0} ((x - s_x)^2 + (y - s_y)^2) - \min_{s \in S_1} ((x - s_x)^2 + (y - s_y)^2) \right) \quad (28)$$

Where $x+jy$ is the received signal point, σ^2 is the inband noise variance, b is one of the k bits of (M -ary) symbol and s_x, s_y is the in-phase and quadrature component of

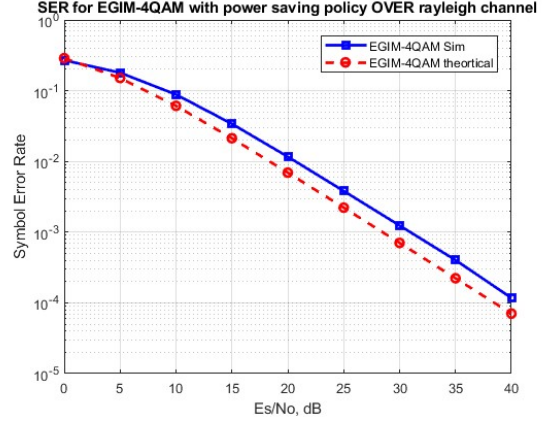


Fig. 8. SER of EGIM-4QAM Versus theoretical bound at $SE \geq 2$ bit

the true constellation points.

In soft decision the Euclidean distance is used as a metric of the decision of the survivor branch on the trellis instead of Hamming distance used in hard decision.

V. SIMULATION RESULTS

TABLE V
SIMULATION PARAMETERS

Parameters	value
Framework	Matlab 2024Ra
Mapping	4QAM, 8PSK
FFT	64
cyclic prefix	16
channel	Rayleigh, AWGN(coded)
number of taps	10
equalizer	MMSE
detector	ML
Traceback Length	12
Constraint Length	4

In this section, we will deduce Matlab simulation results for what had driven in sections III-B and III-C, the error performance for EGIM-4QAM and EGIM-8PSK will be demonstrated in terms of Symbol Error Rate(SER), compared with their theoretical SER upper bound, also the bit error rate of the OFDM-IM autoencoder. The performance of hard and soft decision Viterbi algorithm of the autoencoder will be compared with a standard convolutional encoder of rate $\frac{1}{2}$ produces the same number of symbols.

A. Symbol Error Rate of EGIM-4QAM

The simulation in Fig.8 shows the difference between the theoretical upper bound SER driven in equation (22) and simulation of EGIM-4QAM, where the error event introduced will localize within the symbol bounds while involving all possible combination patterns results in higher spectral efficiency as stated in section III-A.

B. Error Performance of EGIM-8PSK

The validation of EGIM-8PSK SER theoretical upper bound stated in equation (23) with simulation is shown in Fig. 9. Where in Fig.10, the BER rate of EGIM-8PSK is compared with DM-OFDM-IM introduced in [12] for the same spectral efficiency (2.5 bits/subcarrier). The comparison revealed the superiority of EGIM-8PSK especially over the low SNR range. The validation of Fig. 9. shows the SER validation between EGIM-8PSK and its theoretical upper bound stated in equation (23). Where in Fig.10. the BER rate of EGIM-8PSK is compared with DM-OFDM-IM introduced in [12] for the same spectral efficiency (2.5 bits/subcarrier). The comparison revealed the superiority of EGIM-8PSK especially over the low SNR range.

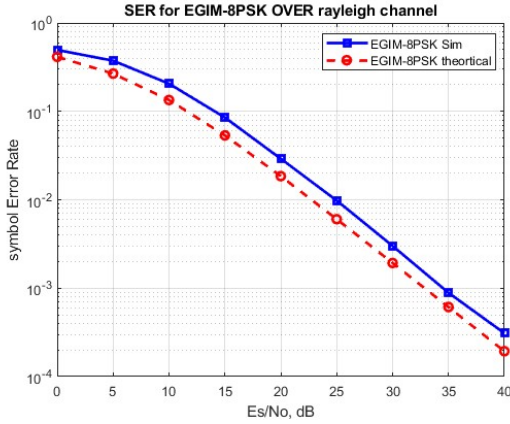


Fig. 9. SER of EGIM-8PSK Versus theoretical bound at $SE \geq 2.5$ bit

C. Performance of proposed Encoder

When compared to a system with the equivalent $Sym_{eff}(R = \frac{1}{2}, 4QAM)$ the proposed convolutional encoder will offer (3dB) enhancement in terms of power efficiency since approximately half of OFDM-IM frame subcarriers are inactive (i.e.: sent with zero power) according to the allowable output symbols of the encoder shown in Fig.7.

The 3dB saved power can be used in two different ways as follows:

- 1) It can be reinvested into the active subcarrier in the OFDM-IM frame, resulting in enhancement of the error performance (0.8dB) in case of soft decision Viterbi decoding while the enhancement will (1.2dB) in the hard decision when compared to a standard encoder of rate $\frac{1}{2}$ as shown in Fig.11.
- 2) Achieving the same error probability with higher order modulation improves spectral efficiency.

The performance of the OFDM-IM autoencoder is tested over the Rayleigh channel using hard and soft decision decoding demonstrated in Fig.12. these results make

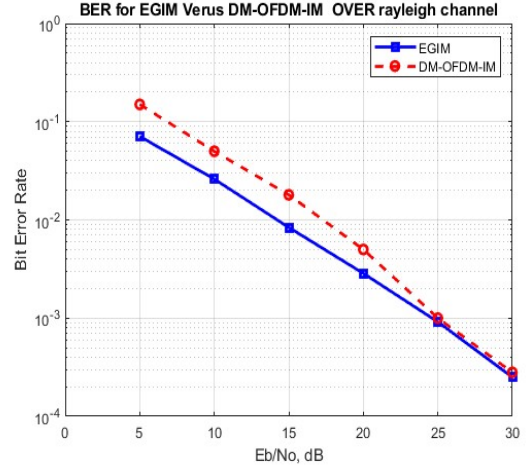


Fig. 10. BER of EGIM-8PSK Versus DM-OFDM-IM at $SE \geq 2.5$ bit

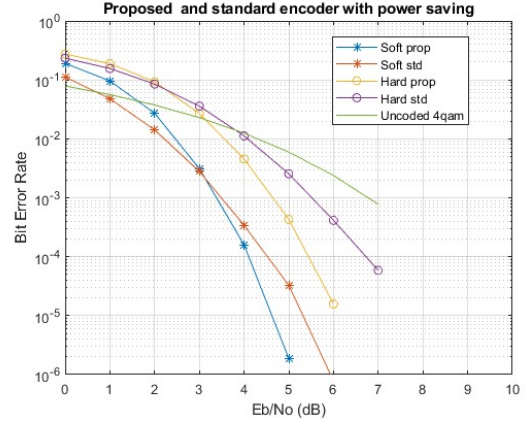


Fig. 11. The Error Performance of OFDM-IM autoencoder with power reinvesting policy over AWGN

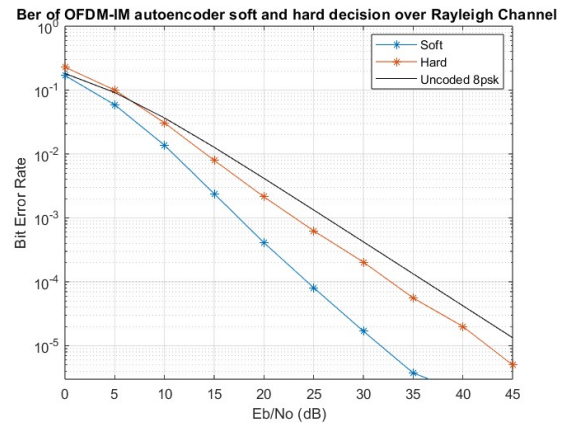


Fig. 12. Ber of OFDM-IM autoencoder soft and hard decision over Rayleigh Channel

sure of the autoencoder's robustness against the channel conditions. The simulations show that the proposed encoder eliminates the chance of the error propagation phenomena that occur when using index modulation with

variable active indices over high-order modulation.

VI. CONCLUSION AND FUTURE WORK

A novel proposed technique for systematically generating and detecting OFDM-IM has been presented. The effect of this technique is studied through two case studies (4QAM-8PSK). Making full use of the whole span over the OFDM-IM frame without splitting reducing transmitter complexity, and involving all possible combination patterns results in enhancement in spectral efficiency per subcarrier without introducing extra computational complexity into the receiver ML detector. The symbol error rates upper bound for (4QAM-8PSK) were driven, and the simulation of both techniques coverage their theoretical bounds. An error propagation OFDM-IM autoencoder was presented to generate pattern combinations in addition to the transmitted bit stream through a special design of a convolutional encoder. The nonlinearity added to the convolutional encoder to generate active and inactive symbols has a 3dB power efficiency gain at the expense of the encoder-free distance which affects its overall error performance.

In the future, one of the main challenges is to enhance the performance of the OFDM-IM autoencoder, achieving almost the standard coding error performance while maintaining the 3dB power efficiency gain or using different channel coding methods to achieve the same concept.

ACKNOWLEDGMENTS

The authors would like to thank the anonymous reviewers for valuable comments that have led to improvements in this paper.

REFERENCES

- [1] E. Başar, Ü. Aygözü, E. Panayırçı, and H. V. Poor, "Orthogonal frequency division multiplexing with index modulation," *IEEE Transactions on signal processing*, vol. 61, no. 22, pp. 5536–5549, 2013.
- [2] R. Abu-Alhiga and H. Haas, "Subcarrier-index modulation ofdm," in *2009 IEEE 20th International Symposium on Personal, Indoor and Mobile Radio Communications*. IEEE, 2009, pp. 177–181.
- [3] D. Tsonev, S. Sinanovic, and H. Haas, "Enhanced subcarrier index modulation (sim) ofdm," in *2011 IEEE GLOBECOM Workshops (GC Wkshps)*. IEEE, 2011, pp. 728–732.
- [4] E. Basar, "Index modulation techniques for 5g wireless networks," *IEEE Communications Magazine*, vol. 54, no. 7, pp. 168–175, 2016.
- [5] E. Başar, "Index modulation: A promising technique for 5g and beyond wireless networks," in *Networks of the Future*. Chapman and Hall/CRC, 2017, pp. 145–166.
- [6] R. Fan, Y. J. Yu, and Y. L. Guan, "Generalization of orthogonal frequency division multiplexing with index modulation," *IEEE transactions on wireless communications*, vol. 14, no. 10, pp. 5350–5359, 2015.
- [7] B. Zheng, F. Chen, M. Wen, F. Ji, H. Yu, and Y. Liu, "Low-complexity ml detector and performance analysis for ofdm with in-phase/quadrature index modulation," *IEEE Communications Letters*, vol. 19, no. 11, pp. 1893–1896, 2015.
- [8] M. Wen, X. Cheng, and L. Yang, *Index modulation for 5G wireless communications*. Springer, 2017, vol. 52.
- [9] S.-Y. Zhang and B. Shahrava, "Polar-coded ofdm with index modulation," *IEEE Access*, vol. 9, pp. 237–247, 2020.
- [10] M. Wen, B. Ye, E. Basar, Q. Li, and F. Ji, "Enhanced orthogonal frequency division multiplexing with index modulation," *IEEE Transactions on Wireless Communications*, vol. 16, no. 7, pp. 4786–4801, 2017.
- [11] X. Yang, Z. Zhang, P. Fu, and J. Zhang, "Spectrum-efficient index modulation with improved constellation mapping," in *2015 International Workshop on High Mobility Wireless Communications (HMWC)*. IEEE, 2015, pp. 91–95.
- [12] T. Mao, Z. Wang, Q. Wang, S. Chen, and L. Hanzo, "Dual-mode index modulation aided ofdm," *IEEE Access*, vol. 5, pp. 50–60, 2016.
- [13] K.-H. Kim and H. Park, "New design of constellation and bit mapping for dual mode ofdm-im," *IEEE Access*, vol. 7, pp. 52573–52580, 2019.
- [14] I. Sengupta, S. Dasgupta, and A. Das Barman, "Generalized index and mode modulated ofdm with improved spectral and energy efficiency," *Transactions on Emerging Telecommunications Technologies*, vol. 35, no. 4, p. e4973, 2024.
- [15] M.-S. Alouini and A. J. Goldsmith, "A unified approach for calculating error rates of linearly modulated signals over generalized fading channels," *IEEE Transactions on Communications*, vol. 47, no. 9, pp. 1324–1334, 1999.
- [16] J. Lassing, E. G. Ström, E. Agrell, and T. Otsson, "Bit error probability of coherent m-ary psk over flat rayleigh fading channels," *Electronics Letters*, vol. 41, no. 21, pp. 1186–1187, 2005.
- [17] M. Abdullahi, A. Cao, A. Zafar, P. Xiao, and I. A. Hemadeh, "A generalized bit error rate evaluation for index modulation based ofdm system," *IEEE Access*, vol. 8, pp. 70082–70094, 2020.
- [18] A. J. Viterbi, "An intuitive justification and a simplified implementation of the map decoder for convolutional codes," *IEEE Journal on Selected Areas in Communications*, vol. 16, no. 2, pp. 260–264, 1998.